Drug Design, Development and Therapy

Dovepress
open access to scientific and medical research

Open Access Full Text Article

ORIGINAL RESEARCH

Inhibition of Axitinib on Buspirone Metabolism in vitro and in vivo

Bo-Wen Zhang[1], Ni-Hong Pang[2], Ren-Ai Xu[1], Gao-Er Qu[3], Cong-Rong Tang[1]

[1]Department of Pharmacy, The First Affiliated Hospital of Wenzhou Medical University, Wenzhou, People's Republic of China; [2]Department of Pharmacy, The Third Affiliated Hospital of Shanghai University (Wenzhou People's Hospital), Wenzhou, People's Republic of China; [3]Department of Pharmacy, Health Service Community of Yueqing Third People's Hospital, Wenzhou, People's Republic of China

Correspondence: Cong-Rong Tang, Department of Pharmacy, The First Affiliated Hospital of Wenzhou Medical University, Wenzhou, People's Republic of China, Tel +86 13867722688, Email 13867722688@163.com

Objective: To evaluate the effect of axitinib on buspirone metabolism in vitro and in vivo.

Methods: A microsome incubation assay was performed to study the effect and mechanism of axitinib on buspirone metabolizing. In vivo, buspirone was administered with or without axitinib to Sprague–Dawley rats. Plasma samples were collected and subjected to ultra-performance liquid chromatography–tandem mass spectrometry.

Results: In both human liver microsomes (HLMs) and rat liver microsomes (RLMs), axitinib (100 μM) decreased buspirone hydroxylation and N-dealkylation by >85%. Axitinib inhibited buspirone hydroxylation and N-dealkylation, with an IC_{50} of 15.76 and 9.74 for RLMs, and 10.63 and 9.902 for HLMs. Axitinib showed noncompetitive inhibition of both 6′-hydroxylation and N-dealkylation. Moreover, coadministration of axitinib and buspirone led to an increase in the maximum plasma concentration (C_{max}) and area under the plasma concentration-time curve (AUC) of buspirone by 4.3- and 5.3-fold, respectively, compared with the control group.

Conclusion: Axitinib inhibited buspirone metabolism in vivo and in vitro, which increases the risk of the side effects of buspirone in the clinic. When coadministered with axitinib, a lower dosage of buspirone should be defined to avoid a toxic response. Axitinib is suspected to function as an inhibitor of CYP3A4.

Keywords: buspirone, axitinib, drug-drug interactions, liver microsomes, noncompetitive inhibition

Introduction

Anxiety is acknowledged as being one of the most common mental diseases, with an incidence of 15–20% and higher morbidity in China, as estimated by experts.[1] Buspirone, a clinical nonbenzodiazepine anti-anxiety agent, has good efficacy in treating anxiety with a low rate of side effects.[2,3] As a partial agonist of 5-HT_{1A}, buspirone was first approved to treat generalized anxiety disorder (GAD) in adults. Buspirone shows better compliance due to its decreased side-effect profile compared to other anxiolytic treatments, especially in patients who do not tolerate the side effects of selective serotonin reuptake inhibitors (SSRIs).[2,4] Unlike benzodiazepines or barbiturates, the pharmacological mechanism of buspirone does not depend on gamma-aminobutyric acid (GABA) receptors; thus, addiction or withdrawal symptoms are uncommon. However, some factors can exacerbate the severe toxic effects of buspirone, such as its combination with ritonavir. Indeed, one patient presented with Parkinson-like symptoms after administration of these two drugs.[5] Moreover, a coadministration method improved the $AUC_{(0\text{-inf})}$ of buspirone to 12.8-fold in a rat model compared to the administration of buspirone only.[6] Increasing novel indications for buspirone have been discovered recently, such as dementia with behavioral disturbance, autism spectrum disorder, and chronic schizophrenia, leading to increased use of buspirone.[7–10] In the clinic, more than 2 weeks of buspirone administration is expected to achieve the desired effect, which increases the probability of long-term medication and the risk of buspirone accumulation. Therefore, further research on buspirone in vivo processes should be advocated.

The progression of chronic physical conditions, such as cancer, is closely related to chronic mental disorders, such as anxiety.[11–13] Cancer has significant psychosocial implications that affect an individual's psychological and spiritual state, and often co-occurs with anxiety in patients.[14–16] According to previous reviews, approximately 90% of renal tumors are renal

Received: 21 January 2022
Accepted: 17 June 2022
Published: 30 June 2022

cell carcinomas (RCC) with a high metastasis risk factor.[17] Vascular endothelial growth factor (VEGF)/VEGF receptor (VEGFR) signaling pathways adjust the function of vessels and play key roles in tumor growth and progression.[18] Axitinib, an inhibitor of VEGFR-1 to 3, is an important drug for advanced RCC. Considering that patients with RCC tend to have a higher rate of psychological disorders, especially anxiety, the use of buspirone combined with axitinib is increased in this patient group. Unfortunately, the risk or benefits of coadministration have never been reported. We studied the effects of axitinib on buspirone metabolism both in vitro and in vivo to provide a useful reference for the clinic.

Buspirone is primarily metabolized by CYP3A, specifically by CYP3A4. The analysis of the main metabolites of buspirone in incubation, including recombinant CYP3A4, demonstrated that 6′-hydroxy buspirone (6′-OH buspirone) and 1-(2-pyrimidyl)-piperazine (1-PP) were the most abundant metabolites, the structures of which are shown in Figure 1.[19] Studies have shown that incubation with microsomes and in vivo pharmacokinetics assays are appropriate methods to evaluate drug-drug interactions (DDIs).[6,20–23] Therefore, we systematically examined the effect of axitinib in human and rat liver microsomes (HLMs and RLMs) in vitro and in Sprague–Dawley (SD) rats in vivo by ultra-performance liquid chromatography–tandem mass spectrometry (UPLC-MS/MS).

Method

Materials and Chemicals

Buspirone hydrochloride (8-(4-(4-(2-pyrimidinyl)-1-piperizinyl) butyl)-8-azaspiro(4,5)decane-7,9-dione) and its main metabolites, including 6′-OH buspirone and 1-PP, were obtained from Heowns Biochem LLC (Tianjin, China); axitinib was purchased from Beijing Sunflower and Technology Development Co., Ltd. (Beijing, China); midazolam (MDZL) and carbamazepine (CBZ) (used as internal standards (IS) in vivo and in vitro, respectively) were purchased from Jiangsu Nhwa Pharmaceutical Co. Ltd. (Jiangsu, China), and Dr. Ehrenstorfer GmbH (Germany), respectively; RLMs and HLMs were purchased from Beijing Sunflower and Technology Development Co. Ltd. (Beijing, China); acetonitrile and methanol of HPLC grade were provided by Merck (Darmstadt, Germany); the nicotinamide adenine dinucleotide phosphate (NADPH)-regenerating system was purchased from Roche (Basel, Sweden); and 1× phosphate-buffered saline (PBS) was purchased from Beyotime Biotechnology Co. (Shanghai, China). All other reagents were of analytical grade purchased from Merck (Darmstadt, Germany).

Instrumentation

The determination of the concentration of buspirone and its main metabolites was conducted by UPLC-MS/MS, consisting of a Waters Acquity I-Class with BEH C18 column (2.1*50 mm) and a Waters Xevo TQD triple-quadrupole mass spectrometer (Waters Corp., Milford, MA, USA) with an electrospray ionization (ESI) source to test and quantify samples. Data were acquired using Masslynx 4.1 software (Waters Corp.).

Michaelis–Menten Curve

The incubation system was designed as buspirone in a 200-μL reaction solution, containing buspirone solubilized in methanol and serially diluted to 5, 10, 20, 50, 100, and 200 μM in PBS buffer (n = 3). RLMs (40 μg) or HLMs (60 μg) were added to take part in this in vitro reaction. After incubation for 5 min at 37°C, the reactions were initiated by the addition of 10 μL of 20 mM NADPH to the samples, which were then incubated at 37°C for 40 min. Next, 400-μL acetonitrile was added to denature the proteins and terminate the incubation. Following addition of 20 μL of 20 ng/mL CBZ as an IS, the tubes were vortexed vigorously for 2 min and centrifuged at 13,000 rpm for 10 min. The supernatant was transferred to a 1.5-mL clean tube and evaluated by UPLC-MS/MS.

Effects of Axitinib on the Metabolism of Buspirone in HLMs and RLMs

The 200-μL incubation consisted of buspirone at a concentration close to the K_m value (50 μM for RLMs or 100 μM for HLMs), RLMs (40 μg) or HLMs (60 μg), and axitinib (0, 0.01, 0.1, 1, 5, 10, 50, and 100 μM), in 1× PBS buffer (n = 3). The samples were preincubated for 5 min, before adding NADPH to start the reactions. After a 40-min incubation at 37°C, the reactions were terminated with 400 μL acetonitrile and 20 μL of 20 ng/mL CBZ (as the IS). After mixing for 2

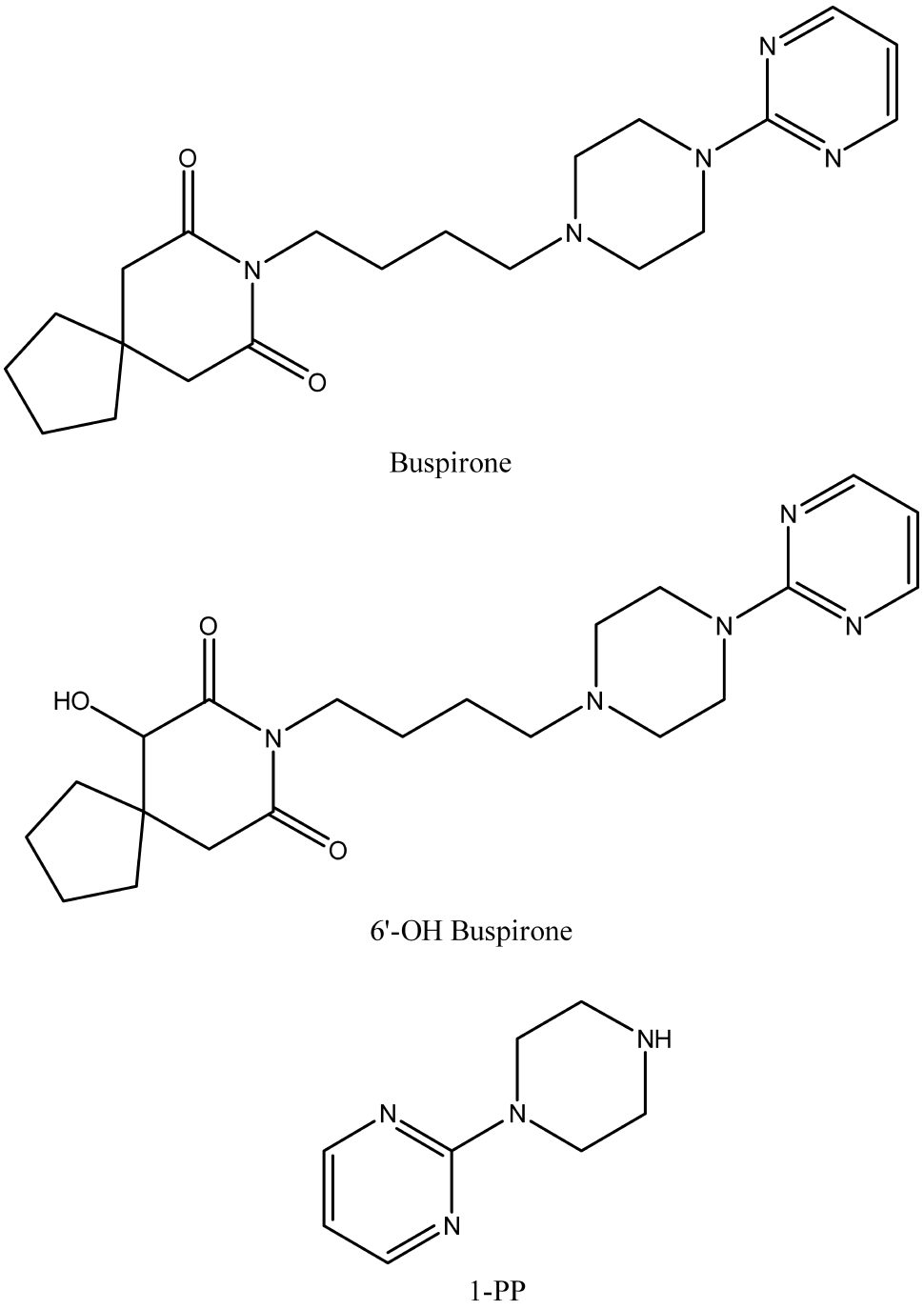

Figure 1 Chemical structures of buspirone, 6′-OH buspirone, and 1-PP.

min and centrifuging at 13,000 rpm for 10 min, the samples were subjected to UPLC-MS/MS analysis to quantify buspirone 6′-hydroxylation and N-dealkylation.

Effects of Axitinib on the Metabolism of Buspirone in Rats in vivo

We purchased 12 male SD rats (approximately 250–300 g) from the Laboratory Animal Centre of Wenzhou Medical University (Wenzhou, China; animal number: 2020-078). The animals were allowed to adapt to laboratory conditions and were provided with sufficient food and water for more than 2 weeks. All procedures conformed to the Guide for the Care

and Use of Laboratory Animals and were conducted with the approval of the Animal Care and Use Committee of Wenzhou Medical University (wydw2020-3022).

The animals were randomly placed into two groups: the control group (A) and the experimental group (B). The animals in both groups were fasted for 12 h before administration (with sufficient water); the B group was administered axitinib distributed in 0.5% carboxymethyl cellulose (CMC) (1 mg/kg) by gavage, and the A group was treated with 0.5% CMC using the same administration approach. After 30 min, the rats in both groups were administered buspirone dissolved in ultrapure water (20 mg/kg) by gavage. Blood samples were collected from the caudal vein at 0, 0.083, 0.167, 0.25, 0.5, 1, 2, 3, 4, 6, 8, 12, and 24 h postdosing. After centrifuging at 13,000 rpm for 10 min, 100-μL plasma samples were extracted from the blood and mixed with a 300-μL aliquot of acetonitrile and a 20-μL aliquot of 200 ng/mL MDZL (IS). After 2 min of vortex mixing and 15 min of centrifugation at 13,000 rpm, the supernatants were collected and diluted with ultrapure water at a ratio of 1:10. The mixtures were subjected to UPLC-MS/MS analysis.

Enzymatic Kinetics of Axitinib Inhibition of Buspirone in RLMs

The incubation was established with buspirone (5–50 μM, which includes the K_m value) as the substrate, axitinib (0–30 μM, which includes the IC_{50} value), and RLMs (40 μg) in 1× PBS buffer. After a 5-min-preincubation at 37°C, the samples were incubated with the addition of 10 μL of 20 mM NADPH at 37°C for 40 min. The method of sample processing was the same as that outlined for the method in Effects of Axitinib on the Metabolism of Buspirone in Rats in vivo.

UPLC-MS/MS

Compounds were separated using a gradient elution method, operating at a flow rate of 0.4 mL/min. The mobile phase consisted of 0.1% formic acid diluted in ultrapure water (as solvent A) and acetonitrile (as solvent B); the solution was held at 10% B for 0.5 min, followed by a linear increase to 98% B at 0.6 min, held at 98% B until 1.1 min, and then ramped back to 10% B at 2.1 min and maintained at 10% B for 0.9 min.

These analytes were detected with an ESI source in multiple reaction monitoring (MRM) mode using the following method: as the desolvation gas, nitrogen was selected to deionize samples at 1000 L h-1, with a desolvation temperature of 600°C. MRM modes were employed for quantification as follows: m/z 386.3 → 122 using a cone voltage (CV) of 20 V and a collision energy (CE) of 30 V for buspirone quantification; m/z 165.1 → 122 using a CV of 20 V and a CE of 15 V for 1-PP; m/z 402.2 → 122 using a CV of 20 V and a CE of 30 V for 6′-OH buspirone; m/z 237.1 → 194.1 using a CV of 10 V and a CE of 20 V for CBZ; and m/z 326.1 → 291.1 using a CV of 10 V and a CE of 25 V for MDZL.

Data Analysis

All results are expressed as the mean ± SD. Michaelis–Menten curves of buspirone, dose response-inhibition curves, drug concentration-time profiles, and enzyme kinetics were constructed and analyzed by GraphPad Prism 5.0 software. We performed the statistical analysis with SPSS 20.0 software using an independent sample *t*-test. P-values <0.05 (in two-tailed test) indicate significant differences between the two groups.

Results

According to chromatogram and mass spectrum data, buspirone and its main metabolites could be separated and detected by this method. Referring to the Michaelis–Menten curve in microsomes (Figure 2), buspirone was metabolized with a K_m of 22.97 μM for 6′-OH buspirone and a K_m of 26.29 μM for 1-PP in RLMs, and with a K_m of 29.37 μM for 6′-OH buspirone and a K_m of 33.55 μM for 1-PP in HLMs. Based on the enzyme kinetic parameters of buspirone, the proper concentration of buspirone was validated for further study in vitro. As shown in Figure 3, in the 6′-hydroxylation pathway, axitinib (100 μM) inhibited 97.4% and 87.4% of buspirone metabolism in RLMs and HLMs, respectively. In N-dealkylation of buspirone, axitinib inhibited 98.4% of buspirone in RLMs and 89.7% in HLMs. The metabolism rate of buspirone in the presence of axitinib was significantly different compared with the control. The curve of dose-response inhibition (Figure 4) showed that axitinib inhibited buspirone metabolism, with IC_{50} values of 15.76 μM for 6′-OH buspirone and 9.74 μM for 1-PP in RLMs, and with IC_{50} values of 10.63 μM for 6′-OH buspirone and 9.902 μM for 1-PP in HLMs.

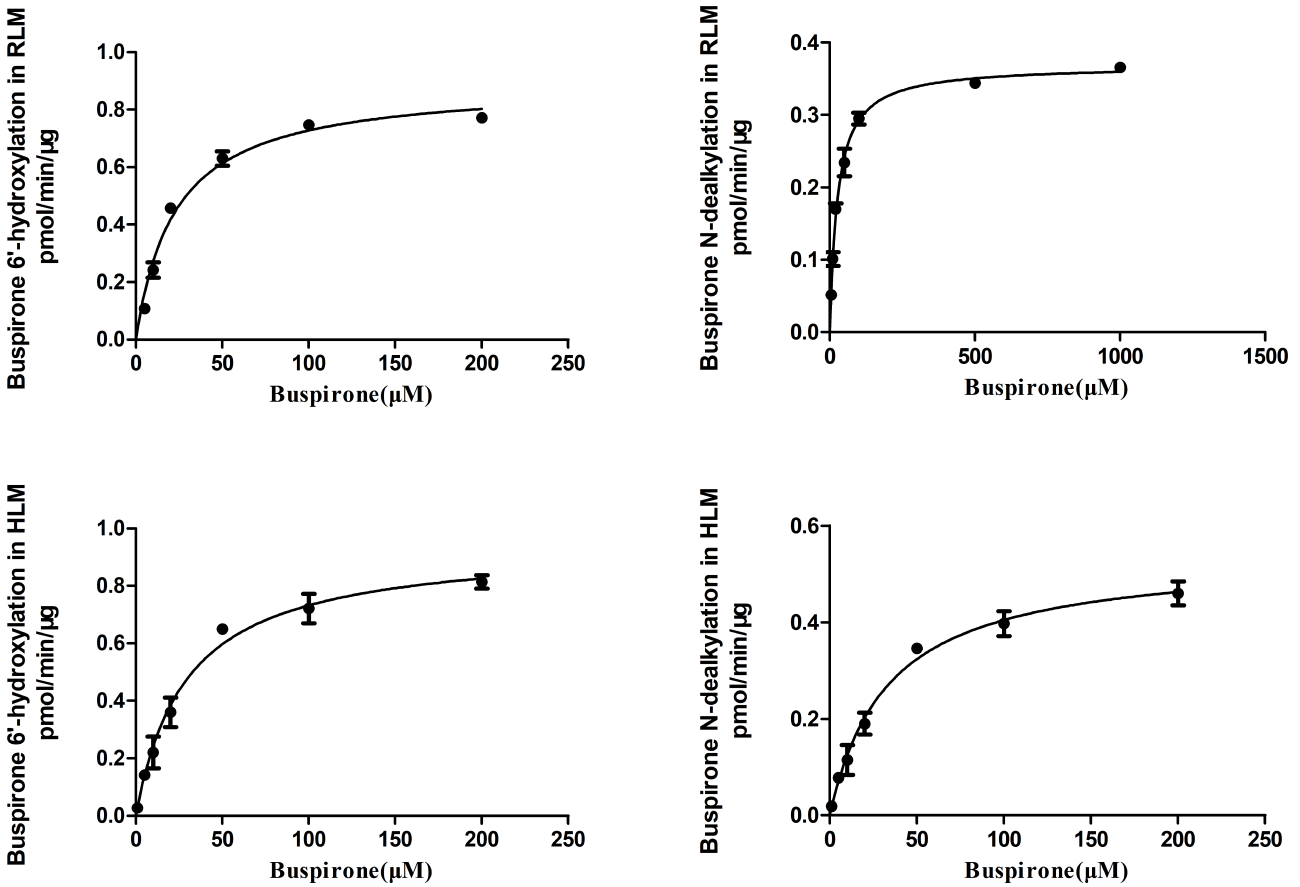

Figure 2 Michaelis–Menten curves for the enzymatic activity of rat and human liver microsomes toward buspirone 6′-hydroxylation and N-dealkylation. Values are presented as the mean ± SD of three replicates.

Figure 5 shows the concentration-time curves of groups A and B, which were graphed with the plasma concentration at the designed time points and the main relevant parameters were obtained (Tables 1–3). The data and curves showed significant differences in the $AUC_{(0\text{-}t)}$, T_{max}, and C_{max}, with mild differences in other indicators between groups A and B. Compared with group A, group B increased the $AUC_{(0\text{-}t)}$ of buspirone to 530%, the T_{max} to 150%, and the C_{max} to 420%. The $AUC_{(0\text{-}t)}$ and $AUC_{(0\text{-}\infty)}$ values for 6′-OH buspirone were significantly higher in group B (2.4-fold) compared with those in the control. The V_z/F and CL_z/F values for 6′-OH buspirone were significantly lower (decreased by 82.3% and 57.2%, respectively) in group B. The T_{max} value of 1-PP in group B was slightly higher than that in the control group. We did not observe any significant differences in the other pharmacokinetic parameters of buspirone and its main metabolites between the two groups.

To study the inhibition pattern, we analyzed the enzymatic kinetics of axitinib inhibition on buspirone in RLMs following incubation with RLMs. As shown in Figure 6, axitinib was determined to be a noncompetitive inhibitor that altered the buspirone metabolism, with a K_i of 4.462 and an α value of 2.139 in the 6′-hydroxylation, and a K_i of 2.606 and an α value of 5.434 in N-dealkylation.

Discussion

It is necessary to study the effects of drugs on buspirone metabolism, although data on buspirone is currently lacking in the literature. Although buspirone is well tolerated in the clinic as an anti-anxiety drug, its accumulation can induce serious reactions to the nervous system.[5] According to a report from Canada, ritonavir is proven to inhibit the metabolism of buspirone in vitro and in vivo.[6] In our pharmacokinetic pre-experiment, the rats were administered ritonavir (the positive inhibitor) before buspirone, and plasma samples were collected at various points postdosing. The results showed

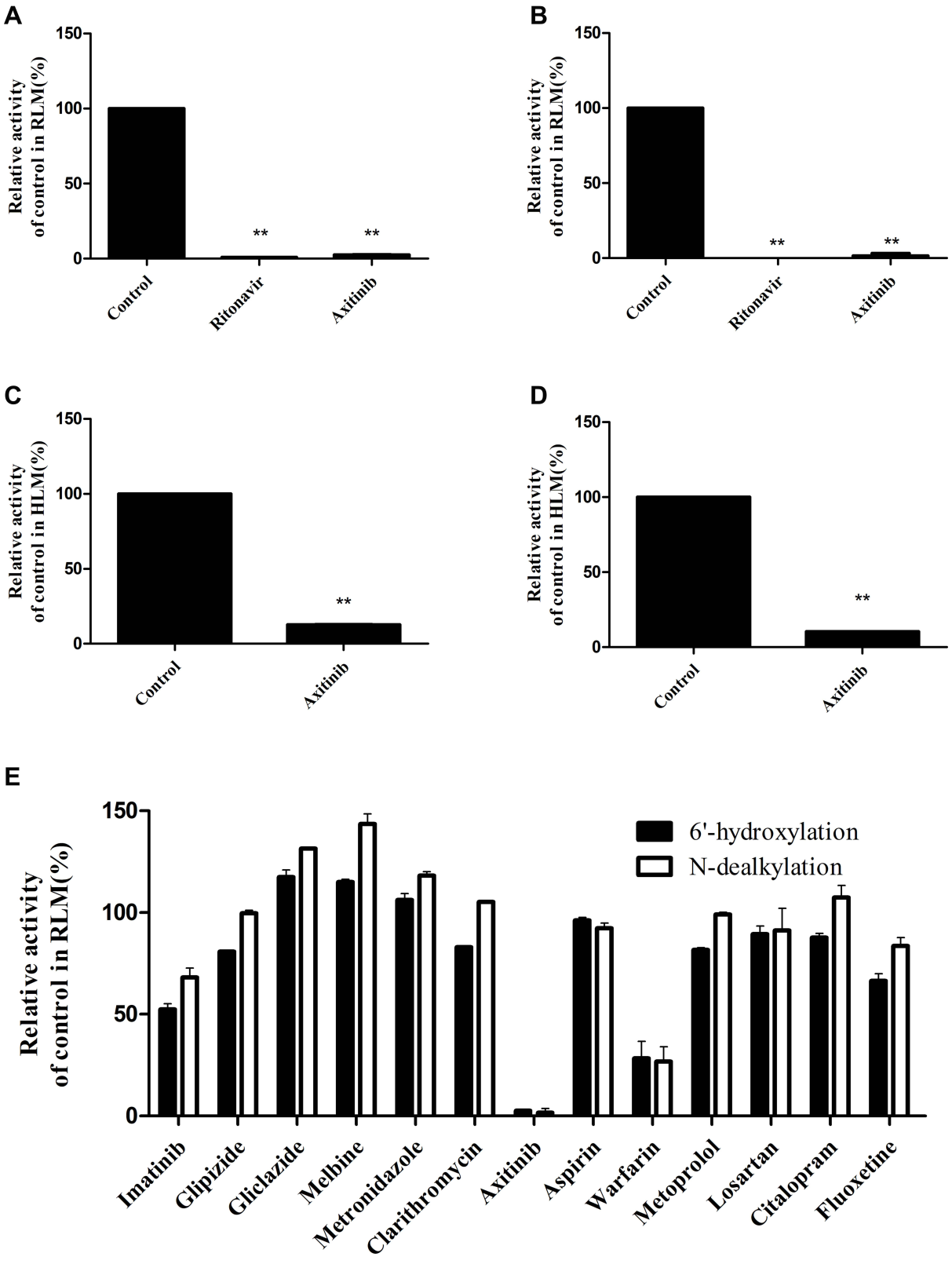

Figure 3 Effect of axitinib (100 μM) on buspirone in the two main metabolic pathways with the addition of rat and human liver microsomes. Part (**A**) and (**C**), Metabolic activity of buspirone in 6′-hydroxylation. Part (**B**) and (**D**), Metabolic activity of buspirone during N-dealkylation. Part (**E**), Effects of common drugs (100 μM) used in the clinic on buspirone metabolism in RLMs. Values are presented as the mean ± SD of three replicates, **P < 0.01 compared to the control.

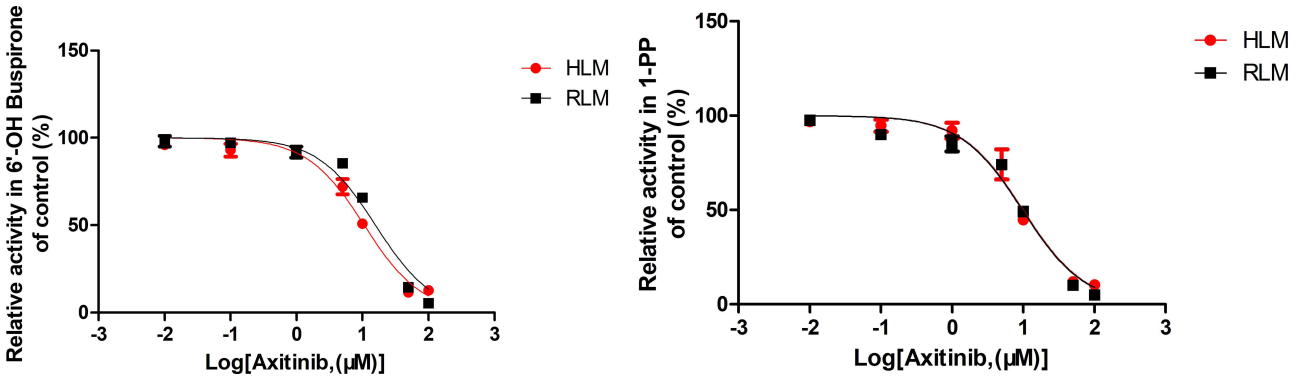

Figure 4 Inhibition of axitinib on buspirone metabolism in the two main pathways, 6′-hydroxylation and N-dealkylation. Values are presented as the mean ± SD of three replicates.

that, compared with the control, the rats showed symptoms of inhibition of respiration and near-death with extremely high blood concentrations of buspirone. The result is consistent with the report that ritonavir inhibits buspirone metabolism,[6] and the accumulation of buspirone can induce serious reactions to the nervous system.[5] Therefore, this method may be useful for studying other drugs that may influence buspirone metabolism.

As shown in this experiment (Figures 3 and 4), axitinib is a potent inhibitor that influences the metabolism of buspirone. Given the results of enzymatic parameters and inhibitory effects, no significant differences in the relative activity were shown between HLMs and RLMs in the presence of various concentrations of axitinib, demonstrating that pharmacokinetic experiments and relevant mechanism studies can be used in rats to evaluate possible interactions in humans. Compared with the control (DMSO) and positive groups (ritonavir, a classical inhibitor to buspirone), axitinib inhibited buspirone metabolism to a large extent, with a similar effect to that experienced in the positive group. More common drugs were selected as the perpetrator drugs to evaluate the inhibition intensity of axitinib according to the method in Effects of Axitinib on the Metabolism of Buspirone in HLMs and RLMs. Compared with the relative activity of the common clinical drugs shown in Figure 3, the inhibitory effect of axitinib on buspirone metabolism was much higher than that of most clinical medicines. Indeed, the IC_{50} (the concentration of axitinib inhibiting half of the original metabolism rate of buspirone) showed strong inhibition of axitinib, which was consistent with the pharmacokinetic results.

It has been reported that axitinib is mainly metabolized by CYP3A4/5, with minor contributions from CYP2C9 and CYP1A2.[19] A 2013 review indicated that axitinib was not an inhibitor of CYP3A4.[19] Another study, however, revealed that axitinib could decrease loperamide intrinsic clearance with an IC_{50} of 1.604 μM in CYP3A4.1 recombinant cell microsomes expressed in Sf-21 cells and showed that axitinib can inhibit loperamide metabolism in CYP3A4.[20]

Additionally, previous US studies have reported that after incubation with CYP450 inhibitor, buspirone metabolism decreased significantly only when the CYP3A4 inhibitor was added.[21] Previous reports have indicated that buspirone is primarily metabolized by CYP3A4 in HLMs, which has been acknowledged as the classical enzymatic substrate of CYP3A4.[21] Given the decreased formation rates of 6′-OH buspirone and 1-PP following the increasing concentration of axitinib (Figure 4), we suspected that axitinib inhibited buspirone metabolism by first inhibiting the enzymatic activity of CYP3A4.

Referring to data from our in vivo experiment (Figure 5), axitinib inhibited buspirone metabolism, significantly increasing the concentrations of buspirone in the plasma and extending the T_{max} in the combined group. As buspirone is rapidly absorbed and has a short half-life value, most time points were designed to be <5 h. Because almost 100% of buspirone was absorbed in the alimentary canal, axitinib could not exert an effect by enhancing absorption; therefore, we focused more on the metabolism. In terms of oral administration, buspirone showed a bioavailability of <5%, which could result from extensive presystemic elimination after absorption. Axitinib can inhibit buspirone metabolism in this process in the liver, meaning that more substrates avoid the first-pass effect and are transferred to the blood. The T_{max} for buspirone was slightly extended in group B, but it unlikely holds any clinical significance because of the small magnitude of the difference. The V_z/F of buspirone was also not significantly improved, which may indicate that axitinib cannot

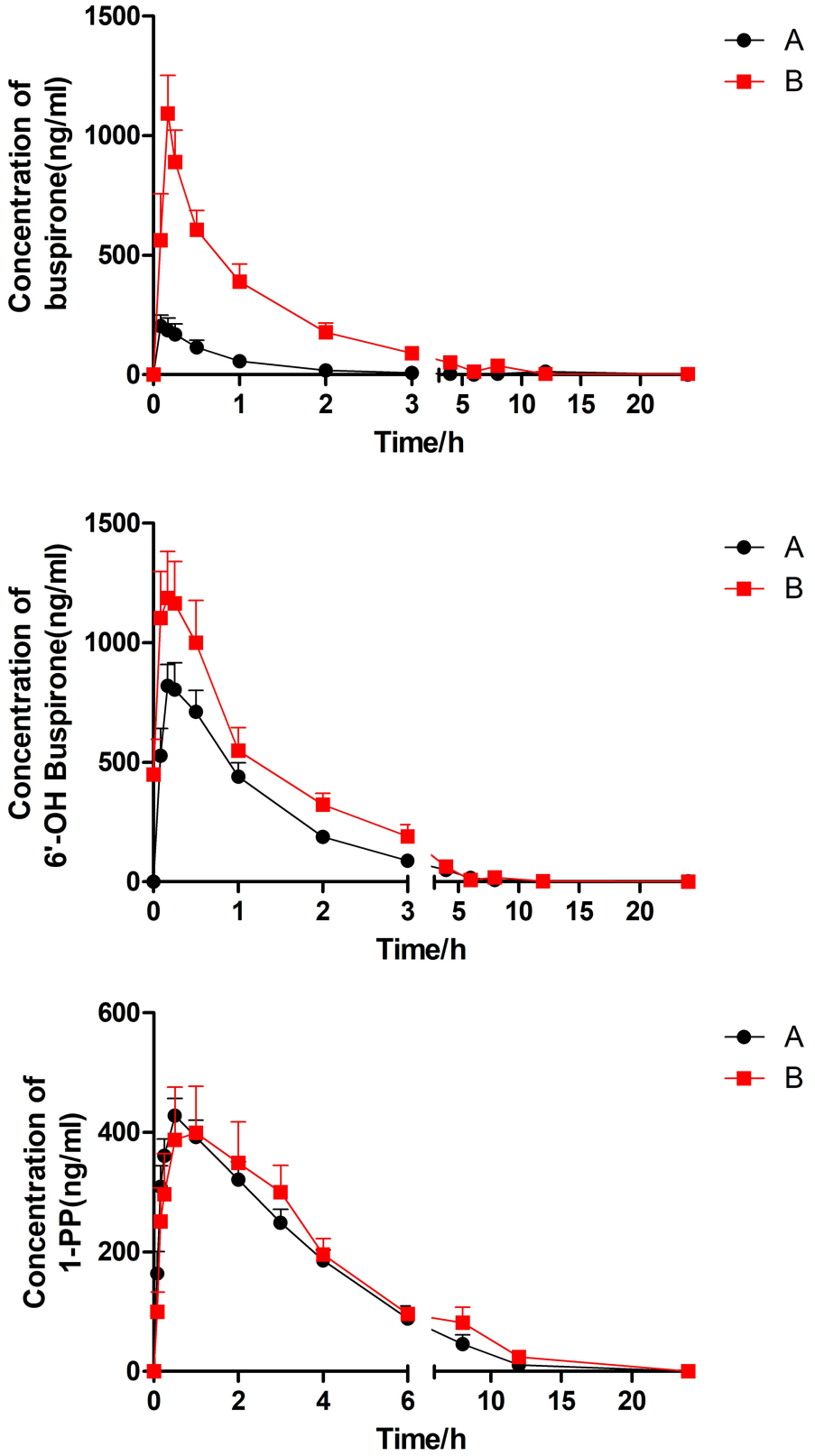

Figure 5 Mean concentration-time curves of buspirone and the two main metabolites (6'-OH buspirone and 1-PP) in groups A and B (n = 6). Values are presented as the mean ± SD.

Table 1 The Main Pharmacokinetic Parameters Were Calculated with Concentration-Time Curves of Buspirone for Both Groups

Parameters	Group A	Group B
$AUC_{(0-t)}$ (μg/L*h)	244.26 ± 89.26	1292.22 ± 462.58*
$AUC_{(0-\infty)}$ (μg/L*h)	2317.54 ± 3206.64	1300.99 ± 455.57
$MRT_{(0-t)}$ (h)	3.64 ± 2.93	2.14 ± 0.86
$MRT_{(0-\infty)}$ (h)	10.25 ± 11.95	2.29 ± 0.86
$t_{1/2z}$ (h)	1.52 ± 0.87	2.41 ± 2.35
T_{max} (h)	0.11 ± 0.04	0.17 ± 0.00*
V_z/F (L/kg)	110.89 ± 107.00	69.71 ± 92.70
CL_z/F (L/h/kg)	60.41 ± 50.74	16.86 ± 5.43
C_{max} (μg/L)	259.96 ± 122.75	1093.10 ± 389.20*

Notes: Values are presented as the mean ± SD measured from six plasma samples of rats. *P < 0.05 compared to the control.

Abbreviations: AUC, Area under the plasma concentration-time curve; MRT, Mean retention time; $t_{1/2z}$, Terminal-phase disposition half-life; T_{max}, Time to reach C_{max}; V_z/F, Clear terminal-phase volume of distribution; CL_z/F, Clearance; C_{max}, Maximum plasma concentration.

Table 2 The Main Pharmacokinetic Parameters Were Calculated with Concentration-Time Curves of 6′-OH Buspirone for Both Groups

Parameters	Group A	Group B
$AUC_{(0-t)}$ (μg/L*h)	1285.60 ± 274.86	3089.26 ± 857.01*
$AUC_{(0-\infty)}$ (μg/L*h)	1296.00 ± 279.97	3092.12 ± 858.13*
$MRT_{(0-t)}$ (h)	1.9 ± 0.73	2.54 ± 1.36
$MRT_{(0-\infty)}$ (h)	2.19 ± 0.99	2.56 ± 1.39
$t_{1/2z}$ (h)	5.90 ± 4.23	2.37 ± 0.62
T_{max} (h)	0.21 ± 0.05	0.46 ± 0.29
V_z/F (L/kg)	130.78 ± 86.85	23.05 ± 6.44*
CL_z/F (L/h/kg)	16.01 ± 3.27	6.86 ± 1.76*
C_{max} (μg/L)	850.23± 237.05	1229.126 ± 471.17

Notes: Values are presented as the mean ± SD measured from six plasma samples of rats. *P < 0.05 compared to the control.

Abbreviations: AUC, Area under the plasma concentration-time curve; MRT, Mean retention time; $t_{1/2z}$, Terminal-phase disposition half-life; T_{max}, Time to reach C_{max}; V_z/F, Clear terminal-phase volume of distribution; CL_z/F, Clearance; C_{max}, Maximum plasma concentration.

Table 3 The Main Pharmacokinetic Parameters Were Calculated with Concentration-Time Curves of 1-PP for Both Groups

Parameters	Group A	Group B
$AUC_{(0-t)}$ (μg/L*h)	1738.84 ± 416.21	2011.26 ± 407.36
$AUC_{(0-\infty)}$ (μg/L*h)	1769.57 ± 443.29	2130.84 ± 390.71
$MRT_{(0-t)}$ (h)	2.99 ± 0.49	3.91 ± 1.66
$MRT_{(0-\infty)}$ (h)	3.16 ± 0.64	4.77 ± 2.95
$t_{1/2z}$ (h)	1.75 ± 0.32	2.74 ± 2.21
T_{max} (h)	0.50 ± 0.00	0.83 ± 0.26*
V_z/F (L/kg)	29.30 ± 5.00	36.90 ± 26.72
CL_z/F (L/h/kg)	11.91 ± 2.94	9.70 ± 2.07
C_{max} (μg/L)	428.27 ± 70.18	432.18 ± 220.18

Notes: Values are presented as the mean ± SD measured from six plasma samples of rats. *P < 0.05 compared to the control.

Abbreviations: AUC, Area under the plasma concentration-time curve; MRT, Mean retention time; $t_{1/2z}$, Terminal-phase disposition half-life; T_{max}, Time to reach C_{max}; V_z/F, Clear terminal-phase volume of distribution; CL_z/F, Clearance; C_{max}, Maximum plasma concentration.

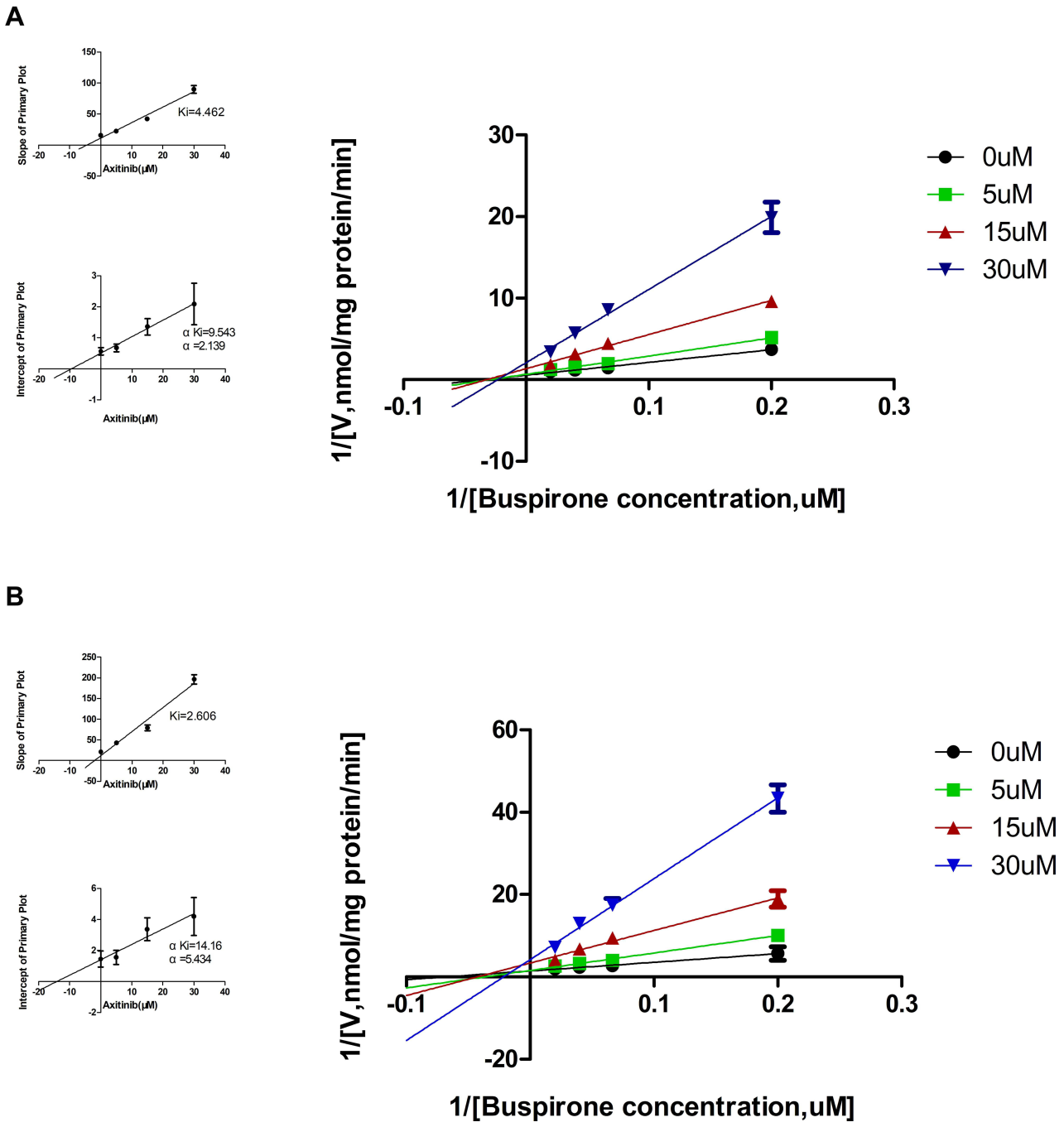

Figure 6 Lineweaver–Burk plot and secondary plots for Ki and α in the inhibition of buspirone metabolism by axitinib (0–30 μM) in RLMs. Part (**A**) represents buspirone 6′-hydroxylation, and part (B) represents buspirone N-dealkylation. Values are presented as the mean ± SD of three replicates.

inhibit buspirone absorption and distribution. The $AUC_{(0-\infty)}$, MRT, $t_{1/2z}$, and CL_z/F for buspirone had no statistical difference between the two groups, which may result from individual differences between rats. As shown in the concentration-time curve and pharmacokinetic parameters (Table 1), coadministration of buspirone with axitinib increased the plasma 6′-OH buspirone concentration (2.4-fold increase in AUC). This may have resulted from the increased plasma buspirone concentration after coadministration with axitinib, which indicated that a large amount of buspirone in the blood could promote metabolism in 6′-hydroxylation. Axitinib also decreased the CL_z/F for 6′-OH buspirone by 57%, and may have inhibited further elimination of the main metabolites. However, no statistically

significant differences in most of pharmacokinetic parameters were observed for 1-PP compared with the control. Although a statistical difference in the T_{max} value for 1-PP was discovered between the two groups, it is unlikely to hold any clinical significance. This may indicate that the blood concentration of buspirone is not the only factor influencing the 1-PP metabolism pathway. Furthermore, as both 6′-OH buspirone and 1-PP are considered to be the major active metabolites of buspirone,[22,23] high concentrations are likely to increase the risk of severe side effects.

To characterize axitinib inhibition on buspirone in rat liver microsomes, various concentrations of inhibitors and substrates were used for enzyme kinetic analysis in vitro. The Lineweaver–Burk plots showed that axitinib noncompetitively inhibited buspirone metabolism and therefore could exert an effect by binding to the inactive sites of hepatic microsomal enzymes. Axitinib did not affect binding of buspirone to liver drug-metabolizing enzymes (especially cytochrome P450), and buspirone had the same K_m value regardless of whether or not axitinib was added. The concentration of buspirone, however, did not influence the axitinib binding these enzymes nor its inhibition.

Conclusion

Axitinib is a potent inhibitor of buspirone metabolism in vivo and in vitro. The interaction between two drugs can induce high blood levels of buspirone, which will greatly increase the risk of drug-induced diseases. Our results demonstrated that pharmacokinetics and microsome incubation assay can be used to evaluate the effect of axitinib on buspirone metabolism in humans. The results also indicated that axitinib is a noncompetitive inhibitor of buspirone metabolism. Axitinib likely exerts an inhibitory effect via CYP3A4. These results suggest that doctors who prescribe the combination of buspirone and axitinib should focus on the severe side effects and dosing strategies of buspirone. If necessary, therapeutic drug monitoring can be conducted to ensure rational drug use.

Acknowledgments

This study was supported by a grant from the Science and Technology Project of Wenzhou (Y20211019). The study was successfully conducted thanks to the assistance of the National Natural Science Foundation of China (NSFC 81973397) and the Special Project of Zhejiang Pharmaceutical Association (2019ZYY37). We thank LetPub for its linguistic assistance during the preparation of this manuscript.

Disclosure

None of the authors declare any conflict of interest regarding this manuscript.

References

1. Shepardson RL, Buchholz LJ, Weisberg RB, et al. Psychological interventions for anxiety in adult primary care patients: a review and recommendations for future research. *J Anxiety Disord*. 2018;54:71–86. doi:10.1016/j.janxdis.2017.12.004
2. Wilson TK, Tripp J. Buspirone. In: *StatPearls*. Treasure Island (FL): StatPearls Publishing StatPearls Publishing LLC.; 2019.
3. Kaur Gill A, Bansal Y, Bhandari R, et al. Gepirone hydrochloride: a novel antidepressant with 5-HT1A agonistic properties. *Drugs Today*. 2019;55(7):423–437. doi:10.1358/dot.2019.55.7.2958474
4. Strawn JR, Mills JA, Cornwall GJ, et al. Buspirone in children and adolescents with anxiety: a review and Bayesian analysis of abandoned randomized controlled trials. *J Child Adolesc Psychopharmacol*. 2018;28(1):2–9. doi:10.1089/cap.2017.0060
5. Clay PG, Adams MM. Pseudo-Parkinson disease secondary to ritonavir-buspirone interaction. *Ann Pharmacother*. 2003;37(2):202–205. doi:10.1177/106002800303700207
6. Rioux N, Bellavance E, Bourg S, et al. Assessment of CYP3A-mediated drug-drug interaction potential for victim drugs using an in vivo rat model. *Biopharm Drug Dispos*. 2013;34(7):396–401. doi:10.1002/bdd.1855
7. Santa Cruz MR, Hidalgo PC, Lee MS, et al. Buspirone for the treatment of dementia with behavioral disturbance. *Int Psychogeriatr*. 2017;29(5):859–862. doi:10.1017/S1041610216002441
8. Chugani DC, Chugani HT, Wiznitzer M, et al. Efficacy of low-dose buspirone for restricted and repetitive behavior in young children with autism spectrum disorder: a randomized trial. *J Pediatr*. 2016;170:45. doi:10.1016/j.jpeds.2015.11.033
9. Goel R, Hong JS, Findling RL, et al. An update on pharmacotherapy of autism spectrum disorder in children and adolescents. *Int Rev Psychiatry*. 2018;30(1):78–95. doi:10.1080/09540261.2018.1458706
10. Ghanizadeh A, Ayoobzadehshirazi A. A randomized double-blind placebo-controlled clinical trial of adjuvant buspirone for irritability in autism. *Pediatr Neurol*. 2015;52(1):77–81. doi:10.1016/j.pediatrneurol.2014.09.017
11. Scott KM, Lim C, Al-Hamzawi A, et al. Association of mental disorders with subsequent chronic physical conditions: world mental health surveys from 17 countries. *JAMA Psychiatry*. 2016;73(2):150–158. doi:10.1001/jamapsychiatry.2015.2688
12. Steel Z, Marnane C, Iranpour C, et al. The global prevalence of common mental disorders: a systematic review and meta-analysis 1980–2013. *Int J Epidemiol*. 2014;43(2):476–493. doi:10.1093/ije/dyu038

13. Dai S, Mo Y, Wang Y, et al. Chronic stress promotes cancer development. *Front Oncol*. 2020;10:1492. doi:10.3389/fonc.2020.01492
14. Yang YL, Liu L, Wang Y, et al. The prevalence of depression and anxiety among Chinese adults with cancer: a systematic review and meta-analysis. *BMC Cancer*. 2013;13:393. doi:10.1186/1471-2407-13-393
15. Zabora J, BrintzenhofeSzoc K, Curbow B, et al. The prevalence of psychological distress by cancer site. *Psychooncology*. 2001;10(1):19–28. doi:10.1002/1099-1611(200101/02)10:1<19::AID-PON501>3.0.CO;2-6
16. Mehnert A, Brähler E, Faller H, et al. Four-week prevalence of mental disorders in patients with cancer across major tumor entities. *J Clin Oncol*. 2014;32(31):3540–3546. doi:10.1200/JCO.2014.56.0086
17. Motzer RJ, Bander NH, Nanus DM. Renal-cell carcinoma. *N Engl J Med*. 1996;335(12):865–875. doi:10.1056/NEJM199609193351207
18. Parekh H, Griswold J, Rini B. Axitinib for the treatment of metastatic renal cell carcinoma. *Future Oncol*. 2016;12(3):303–311. doi:10.2217/fon.15.322
19. Chen Y, Tortorici MA, Garrett M, et al. Clinical pharmacology of axitinib. *Clin Pharmacokinet*. 2013;52(9):713–725. doi:10.1007/s40262-013-0068-3
20. Lin QM, Pang NH, Li YH, et al. Investigation of the effects of axitinib on the pharmacokinetics of loperamide and its main metabolite N-demethylated loperamide in rats by UPLC-MS/MS. *Chem Biol Interact*. 2019;310:108744. doi:10.1016/j.cbi.2019.108744
21. Zhu M, Zhao W, Jimenez H, et al. Cytochrome P450 3A-mediated metabolism of buspirone in human liver microsomes. *Drug Metab Dispos*. 2005;33(4):500–507. doi:10.1124/dmd.104.000836
22. Gammans RE, Mayol RF, LaBudde JA. Metabolism and disposition of buspirone. *Am J Med*. 1986;80(3):41–51. doi:10.1016/0002-9343(86)90331-1
23. Wong H, Dockens RC, Pajor L, et al. 6-hydroxy buspirone is a major active metabolite of buspirone: assessment of pharmacokinetics and 5-hydroxytryptamine1A receptor occupancy in rats. *Drug Metab Dispos*. 2007;35(8):1387–1392. doi:10.1124/dmd.107.015768